Spectrochimica Acta Part A: Molecular and Biomolecular Spectroscopy 146 (2015) 88–96

Contents lists available at ScienceDirect

Spectrochimica Acta Part A: Molecular and Biomolecular Spectroscopy

journal homepage: www.elsevier.com/locate/saa

An investigations on the molecular structure, FT-IR, FT-Raman and NMR spectra of 1-(p-tolylsulfonyl) pyrrole by theoretical and experimental approach

Y. Erdogdu [a,*], S. Saglam [b], M.T. Gulluoglu [a]

[a] Department of Physics, Ahi Evran University, 40040 Kirsehir, Turkey
[b] Department of Physics, Gazi University, 06100 Ankara, Turkey

HIGHLIGHTS

- FT-IR, FT-Raman and FT-NMR spectra of 1-(p-tolylsulfonyl) pyrrole molecule are recorded and analyzed.
- Theoretical approach to spectra based on DFT (B3LYP) method with 6-311 G(d,p), cc-pVDZ, cc-pVTZ and cc-pVQZ basis sets.
- The observed and calculated FT-IR, FT-Raman, ^{13}C NMR chemical shifts are in close agreement.
- All calculations are calculated theoretically using Gaussian 09 and Spartan 10 software.

GRAPHICAL ABSTRACT

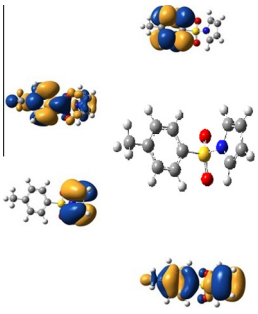

ARTICLE INFO

Article history:
Received 11 November 2014
Received in revised form 29 January 2015
Accepted 1 March 2015
Available online 9 March 2015

Keywords:
1-(p-Tolylsulfonyl) pyrrole
B3LYP
Infrared
Raman and NMR spectra

ABSTRACT

Fourier-Transform-Infrared, Fourier-Transform-Raman and Nuclear Magnetic Rezonans spectra of 1-(p-tolylsulfonyl) pyrrole molecule have been recorded. In the powder form, vibrational spectra of 1-(p-tolylsulfonyl) pyrrol molecule were investigated in the region 4000–400 cm^{-1} and 3500–50 cm^{-1}, respectively. The conformational analysis, geometrical structure, molecular electrostatic potential map, HOMO–LUMO and vibrational spectroscopic properties of the isolated 1-(p-tolylsulfonyl) pyrrole molecule have also been carried out at the Molecular Mechanic and Density Functional Theory approaches. Density Functional Theory results have been associated with Scaled Quantum Mechanics Force Field for fitting between the theoretical and the experimental frequencies.

Introduction

In the conducting polymers (especially polypyrrole (PPy)) constitute an active field of research because of their potential properties such as facilitate of synthesis, good redox properties, stability in the oxidized form. Polypyrrole (PPy) has the high electrical conductivity ability. It has also some unique electrical and optical properties [1–4]. Alp and co-workers investigated that polypyrrole and its derivatives were widely used as pro-drugs. Note that 5-lactams has shown anti-tumour activity in that work. In the recent years, N-substituted maleimides and 5-ylidene pyrrol-2(5H)-ones have been attracted to the great attention [7]. Because, they have the biological activity properties. In addition, it has also potentials usage as key compounds for synthesis of biological molecules such as Oteromycin, Talaroconvolutin A, Azaspirene, Fusarin, Clausenamide [5–7].

The sulfonyl group is bi-functional group. It has provided an excellent freedom in the synthesis of compounds for some advanced applications. It is allows more flexibility for synthetically

* Corresponding author.
E-mail address: yusuferdogdu@gmail.com (Y. Erdogdu).

http://dx.doi.org/10.1016/j.saa.2015.03.031
1386-1425/

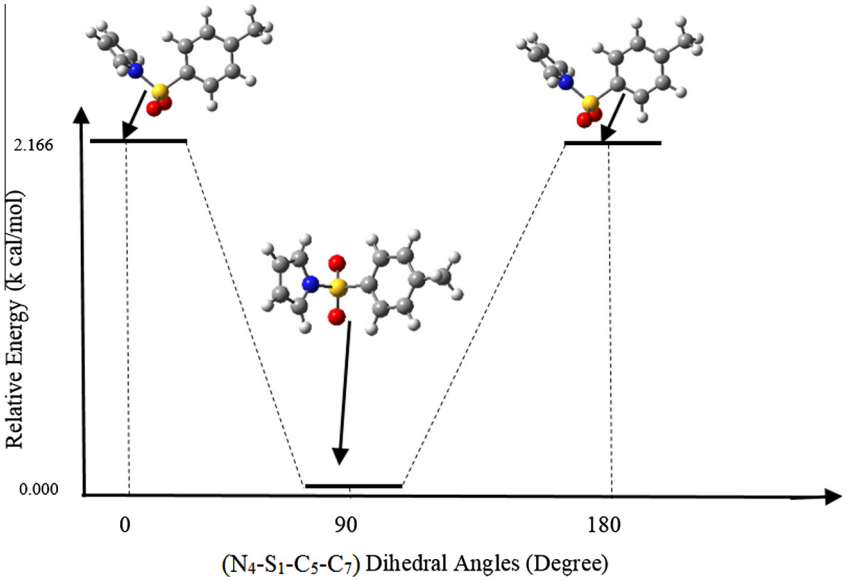

Fig. 1a. Conformational analysis results of 1PTSP molecule.

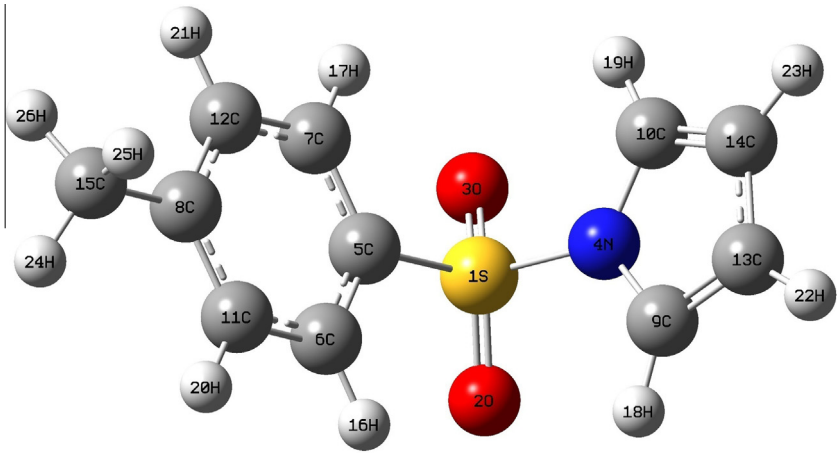

Fig. 1b. Molecular structure and atomic numbering of 1PTSP molecule.

tailoring the physical properties. Comparisons of the nitro and cyanovinyl groups, sulfonyl group has strong acceptor property. If both attached substituent in $-SO_2-$ group are different, asymmetrical molecule result and ultimately leading to variation in properties [8].

Sulfonation is the most important in the industrial for the aromatic compounds due to the availability and low cost of the reagent. Recently, their reaction has been extensively investigated such as major to the syntheses of a multitude of various aromatic sulfonyl derivatives [9].

To characterize 1PTSP by means of Vibrational and Nuclear Magnetic Resonance spectroscopy, it is necessary to perform the complete assignment of the NMR, infrared and Raman spectra, which were unassigned until now. In this context, the goal of this work was to study the structural and vibrational and NMR properties of 1PTSP from the theoretical and experimental points of view through the combination of DFT calculations with vibrational spectra using the Scaled Quantum Mechanics Force Field (SQMFF) methodology. The assignments of the observed and measured wavenumbers were determined by the SQMFF results. The comparisons of the theoretical vibrational and NMR spectra with the corresponding experimental ones demonstrate a good concordance. In the present work, the goal of this work is detail in investigation of the structural and conformational analysis, some spectral analysis (FT-IR, FT-Raman and FT-NMR) by experimental and theoretical procedures.

Experimental

The FT-IR spectrum of 1PTSP molecule was measured (4000–400 cm^{-1}) by using Vertex 80 spectrophotometer. The FT-Raman spectrum of 1PTSP molecule was measured (3500–50 cm^{-1}) by using the Thermo scientific DXR Raman Microscope. It is used at 1064 nm line of Nd: YAG laser as excitation wavelength. The ^{1}H and ^{13}C NMR spectra were recorded by using Bruker Ultra shield FT-NMR Spectrometer. All NMR spectra were measured at room temperature.

Computational procedure

In the present work, DFT/B3LYP approach was employed by using Gaussian 09 software [10,11]. In order to predict conformers of 1PTSP molecule, the conformational space of 1PTSP molecule

Table 1
Computed structural parameters (Å and degree) of 1-(p-tolylsulfonyl) pyrrole.

	B3LYP/6-311 G(d,p)	B3LYP/cc-pVDZ	B3LYP/cc-pVTZ	B3LYP/cc-pVQZ	Exp*
Bond lengths (Å)					
N_4-C_{10}	1.391	1.390	1.384	1.387	
N_4-C_4	1.391	1.390	1.387	1.387	
N_4-S_1	1.715	1.736	1.705	1.696	1.640
S_1-O_2	1.453	1.477	1.446	1.437	1.420
S_1-O_3	1.453	1.477	1.446	1.437	1.430
S_1-C_5	1.790	1.797	1.783	1.777	1.750
C_5-C_6	1.393	1.396	1.389	1.390	1.380
C_7-C_5	1.393	1.396	1.396	1.390	1.390
C_6-C_{11}	1.39	1.394	1.386	1.386	1.370
C_7-C_{12}	1.390	1.394	1.386	1.386	1.380
C_{11}-C_8	1.399	1.404	1.396	1.396	1.390
C_8-C_{15}	1.508	1.508	1.504	1.504	1.510
Bond angle (°)					
N_4-S_1-O_2	105.4	105.0	105.4	105.5	104.7
N_4-S_1-O_3	105.4	105.0	105.4	105.5	106.7
N_4-S_1-C_5	108.5	103.8	104.5	104.6	107.4
S_1-C_5-C_7	119.3	119.2	119.4	119.5	120.0
O_2-S_1-O_3	123.1	123.7	122.5	122.4	119.8
S_1-C_5-C_6	119.3	119.2	119.4	119.5	119.3
C_5-C_7-C_{12}	118.9	118.7	119.0	119.1	119.4
C_5-C_6-C_{11}	118.9	118.7	119.0	119.1	118.8
C_{12}-C_8-C_{15}	120.7	120.7	120.7	120.7	121.3
C_{12}-C_8-C_{11}	118.4	118.4	118.4	118.4	118.4
C_{11}-C_8-C_{15}	120.7	120.7	120.7	120.7	120.2
C_{10}-N_4-S_1	124.9	124.9	124.9	125.0	
C_{10}-N_4-C_9	109.4	109.7	109.3	109.2	
Dihedral angle					
N_4-S_1-C_5-C_7	90.01	90.90	90.25	90.20	−83.01
O_2-S_1-C_5-C_6	21.93	20.56	22.00	22.14	−19.74
S_1-C_5-C_7-C_{12}	−179.6	179.5	179.91	179.91	175.9
C_{12}-C_8-C_{15}-H_{25}	−151.3	−151.4	−151.3	−151.3	120.5
S_1-N_4-C_9-C_3	−172.3	−173.1	−172.1	−171.9	
S_1-N_4-C_9-H_{18}	10.05	8.887	10.03	10.10	

* Taken from Ref. [15].

was searched by semi empirical Merck Molecular Force Field (MMFF) method [12]. The candidate structures were then re-optimized at the DFT/B3LYP level. Frequency calculations were done to confirm that the reported structures are true minima. To predict the spectroscopic properties of the most stable structure, DFT approach was used in the Gaussian software. The computed wavenumbers were scaled with the scaling factor in order to figure out how the predicted vibrational spectra are in agreement with experimental ones. The vibrational modes were assigned from the based on TED analysis. In this step, SQM program used the Gaussian output for B3LYP/6-311 G(d,p) level of theory [13].

Results and discussion

Conformational properties and optimization of molecular geometry

To predict the candidate conformers of 1PTSP molecule, potential energy surface have been scanned by means of the Spartan 10 [14] software at the MMFF. Conformational results were shown in Fig. 1-a.

Most stable conformational geometry of 1PTSP molecule obtained by B3LYP/6-311 G(d,p) basis set as seen in Fig. 1-b. The selected geometrical parameters were listed in Table 1 together with experimental X-ray data. To the best of our knowledge; there are no experimental geometrical parameters of1PTSP molecule. So, we could compare our calculated results with experimental ones of same molecular structure [15].

C–C bond distances were predicted about 1.390 Å for the carbon of the phenyl group and about 1.380 Å for those of the phenyl group by B3LYP/6-311 G(d,p) level of theory. CC Bond distances of pyrrole group were determined shorter than those of phenyl group. CC bond distances with methyl group were calculated larger than other Carbon–Carbon bond distances. This distance were computed at 1.508 Å (B3LYP/6-311 G(d,p)) and at 1.510 Å (X-ray) by theoretical and experimental approaches. Bond angle between phenyl group and pyrrole group is about 90° by optimization and conformational analysis results. This angle were founded at 83.01° by experimental technique. Selected bond lengths, bond angles and dihedral angles were given in Table 1. The molecular structure and atomic numbering was given in Fig. 1 by the B3LYP/6-311 G(d,p) level of theory. The most stable geometry has been used to calculate spectroscopic properties of 1PTSP.

Vibrational analysis

The 1PTSP molecule has 26 atoms ($C_{11}H_{11}NO_2S$), so it has 72 normal modes of vibrations. Vibrational analysis of 1PTSP molecule were computed by using B3LYP level with some basis sets such as 6-311 G(d,p), cc-pVDZ, cc-pVTZ and cc-pVQZ. The detected and predicted vibrational spectrum with TED results of fundamental vibrational modes were given in Table 2. The Fourier Transform Infrared spectra in 4000–400 cm^{-1} region and corresponding Fourier Transform Raman spectra in 3500–350 cm^{-1} region is show in Figs. 2 and 3.

Pyrrole group vibrations

It is note that the CH stretching vibrations are computed between 2927 cm^{-1} and 3175 cm^{-1} by B3LYP/6-311 G(d,p). The CH stretching of pyrrole group vibrations were observed at higher wavenumber region than those of the phenyl group. The pyrrole group has four CH stretching modes, which are C_1H_6, C_2H_7, C_3H_8 and C_4H_9 bonds. The observed CH stretching of pyrrole group at 3229 cm^{-1}, 3148 cm^{-1} and 3120 cm^{-1} corroborate well with theoretical predicted stretching vibrations by means of FT-Raman spectra. These vibrations were predicted pure bands with a TED contribution of about 80%.

Phenyl group vibrations

In this work, the CH stretching modes of the phenyl group was identified as 3031 (Raman) cm^{-1} and 3101 (DFT) cm^{-1}. This mode was assigned to the CH stretching vibration of the phenyl group. Other phenyl group vibrations (mode nos: 67, 66 and 65) could not to be measured by experimental methods.

In the phenyl ring, the in-plane and out-of-plane CH deformations vibrations are expected above and below 1000 cm^{-1}, respectively [17–22]. The in-plane CH deformation modes of the phenyl ring are assigned at 1102 cm^{-1}, 1167 cm^{-1}, 1287 cm^{-1}, 1384 cm^{-1} theoretically (DFT) and at 1290 cm^{-1}, 1358 cm^{-1} in the IR spectrum. The o-o-p (out-of-plane) CH deformations modes have a weaker intensity in high frequencies region, while it can be determined to be higher intensity than those of high frequencies region in lower frequencies region. The CH out-of-plane modes of the phenyl ring are assigned at 953 cm^{-1}, 958 cm^{-1}, 820 cm^{-1} and 797 cm^{-1} theoretically (DFT) and at 726 cm^{-1}, 848 cm^{-1}, 912 cm^{-1}, 970 cm^{-1} in the IR spectrum. The PED predicted that these vibrations are of mixed mode as is evident from Table 2 almost contributing 30–70%.

Methyl group vibrations

In the methyl group, the CH stretching vibrational modes appear at lower frequencies than those of aromatic ring. In addition, the asymmetric stretching modes are usually founded at higher wavenumber than the symmetric ones [16]. 3008 cm^{-1} and

Table 2
Comparasion of computed and measured frequencies (cm^{-1}) of 1-(p-tolylsulfonyl) pyrrole.

Mode no	Theoretical (B3LYP)						Experimental		%TED[d]
	6-311 G(d,p)			cc-pVDZ	cc-pVQZ	cc-pVTZ	FT-IR	FT-Raman	
	Freq[a]	I_{IR}[b]	I_{Raman}[c]	Freq[a]	Freq[a]				
υ_1	3175	1	40	3190	3181	3169		3229	υ_{CH}(78%)
υ_2	3171	1	1	3186	3177	3166			υ_{CH}(78%)
υ_3	3138	3	53	3154	3145	3134	3144	3148	υ_{CH}(82%)
υ_4	3126	3	35	3141	3134	3122		3120	υ_{CH}(80%)
υ_5	3101	1	43	3121	3107	3096		3031	υ_{CH}(78%)
υ_6	3100	0	3	3120	3106	3096			υ_{CH}(79%
υ_7	3067	4	37	3083	3072	3061			υ_{CH}(76%)
υ_8	3066	6	31	3082	3071	3061			υ_{CH}(79%)
υ_9	3008	6	22	3030	3012	3001			υ_{CH}(78%)
υ_{10}	2982	7	33	3000	2985	2974			υ_{CH}(77%)
υ_{11}	2927	9	100	2937	2933	2911		2920	υ_{CH}(89%)
υ_{12}	1584	11	27	1598	1587	1582	1594	1594	δ_{CCH}(39%)+υ_{CC}(33%)++δ_{CCC}(18%)
υ_{13}	1562	0	1	1576	1562	1558			δ_{CCH}(33%)+υ_{CC}(27%)+δ_{CCC}(17%)
υ_{14}	1522	1	0	1528	1524	1519	1537		δ_{CCH}(40%)+υ_{CC}(20%)+δ_{NCH}(12%)
υ_{15}	1474	5	1	1474	1484	1477	1493		δ_{CCH}(58%)+υ_{CC}(23%)
υ_{16}	1443	8	4	1435	1446	1440	1459		τ_{CCCH}(38%)+δ_{CHH}(27%)+δ_{CCH}(18%)
υ_{17}	1442	3	6	1421	1444	1439		1461	τ_{CCCH}(41%)+δ_{CHH}(36%)+δ_{CCH}(14%)
υ_{18}	1429	20	9	1416	1434	1428	1400	1391	δ_{CNH}(22%)+δ_{CCH}(22%)+υ_{CC}(14%)
υ_{19}	1384	4	0	1384	1390	1384	1358		δ_{CCH}(39%)+τ_{CCCH}(16%)+υ_{CC}(14%)+δ_{CCC}(10%)
υ_{20}	1378	0	5	1382	1381	1376			δ_{CCH}(52%)+υ_{CC}(21%)+δ_{CCN}(6%)
υ_{21}	1369	1	10	1354	1373	1368			δ_{CHH}(38%)+δ_{CCH}(34%)+τ_{CCCH}(11%)
υ_{22}	1306	44	1	1316	1339	1322	1309		δ_{CCH}(23%)+υ_{CC}(14%)+υ_{SO}(12%)
υ_{23}	1287	3	0	1300	1299	1293			δ_{CCH}(61%)
υ_{24}	1286	12	8	1274	1286	1283	1290		υ_{CC}(31%)+δ_{CCH}(29%)+τ_{CCCH}(10%)
υ_{25}	1276	8	0	1261	1284	1279			δ_{CCH}(46%)+υ_{CN}(12%)
υ_{26}	1228	1	0	1215	1235	1228			δ_{CCH}(44%)+δ_{CNH}(20%)
υ_{27}	1189	1	4	1197	1193	1189		1174	δ_{CCH}(34%)+υ_{CC}(27%)+δ_{CCC}(21%)
υ_{28}	1167	1	1	1159	1173	1168			δ_{CCH}(68%)+υ_{CC}(15%)
υ_{29}	1156	59	6	1157	1167	1159			δ_{CCH}(29%)+υ_{CC}(12%)+υ_{CN}(10%)
υ_{30}	1103	100	17	1094	1136	1121	1168	1087	υ_{CC}(15%)+δ_{CCH}(14%)+υ_{SO}(13%)
υ_{31}	1102	4	0	1090	1106	1102			δ_{CCH}(59%)+υ_{CC}(11%)
υ_{32}	1057	8	1	1044	1064	1057	1077		δ_{CCH}(65%)
υ_{33}	1050	9	7	1043	1062	1056	1057		δ_{CCH}(29%)+υ_{CC}(18%)
υ_{34}	1036	61	6	1030	1041	1036	1033	1034	δ_{CCH}(36%)
υ_{35}	1028	9	0	1019	1034	1029			τ_{CCCH}(44%)+δ_{CCH}(26%)+τ_{CCCC}(15%)
υ_{36}	1011	48	1	1005	1017	1011	1016		δ_{CCH}(33%)+υ_{CC}(11%)+τ_{CCCH}(11%)
υ_{37}	997	4	0	992	105	1001			δ_{CCH}(28%)+δ_{CCC}(27%)+υ_{CC}(11%)
υ_{38}	977	0	0	972	980	976			τ_{CCCH}(39%)+δ_{CCH}(31%)
υ_{39}	953	0	0	960	967	962			τ_{CCCH}(47%)+τ_{CCHH}(20%)+τ_{CCSH}(10%)+τ_{CCCC}(10%)
υ_{40}	938	0	0	949	955	951			τ_{CCCH}(42%)+τ_{CCHH}(19%)+τ_{CCCC}(13%)+τ_{CCSH}(11%)
υ_{41}	916	0	4	907	924	918	934	935	δ_{CCH}(30%)+δ_{CCN}(15%)
υ_{42}	869	0	0	869	874	871			τ_{CCHH}(27%)+τ_{CCNH}(20%)+τ_{CCCH}(18%)
υ_{43}	852	0	0	846	830	852			δ_{CCC}(22%)+δ_{CCN}(13%)+δ_{CNH}(13%)
υ_{44}	830	0	0	828	843	837			τ_{CCCH}(28%)+τ_{CCHH}(25%)+τ_{CCNH}(10%)
υ_{45}	820	0	1	824	856	826	812	811	τ_{CCCH}(72%)+τ_{CCSH}(14%)
υ_{46}	797	100	2	808	812	809	797		τ_{CCCH}(53%)+τ_{CCSH}(11%)
υ_{47}	786	4	6	788	792	788	754		τ_{CCCH}(33%)+υ_{CC}(11%)
υ_{48}	712	59	2	714	724	720	702		τ_{CCCH}(32%) +τ_{CCNH}(29%)+τ_{CHSN}(16%)
υ_{49}	689	4	5	698	706	703		674	τ_{CCCH}(43%)+τ_{CCCC}(26%)
υ_{50}	672	0	0	673	689	684			τ_{CCCH}(27%)+τ_{CCHH}(20%)+τ_{CCNH}(17%)+τ_{CHSN}(17%)
υ_{51}	642	91	0	631	651	644	670		τ_{CCCH}(11%)+τ_{CNSO}(10%)
υ_{52}	627	0	2	624	631	628			δ_{CCC}(38%)+δ_{CCH}(30%)
υ_{53}	602	0	0	601	601	600			τ_{CCCN}(26%)+ τ_{CCCH}(25%)+τ_{CCCC}(12%)
υ_{54}	583	8	2	579	593	589	597	594	τ_{CCCN}(22%)+τ_{CSNO}(18%)+τ_{CCNH}(12%)+τ_{CCCH}(12%)+τ_{CCNS}(11%)
υ_{55}	568	85	1	556	577	571	586		τ_{CCCH}(20%)+τ_{CCSO}(10%)
υ_{56}	514	24	0	504	525	519			τ_{CCCH}(21%)
υ_{57}	472	0	1	472	482	479			τ_{CCCH}(40%)+τ_{CCCC}(22%)+τ_{CCSO}(11%)
υ_{58}	462	1	0	455	470	465			τ_{CCSO}(18%)+δ_{NSO}(10%)
υ_{59}	401	0	0	404	403	402			τ_{CCCC}(37%)+τ_{CCCH}(35%)
υ_{60}	363	0	1	360	368	364		370	δ_{CCH}(23%)+τ_{CCCH}(15%)
υ_{61}	328	1	0	326	337	331			τ_{CCCH}(24%)+τ_{CCCC}(18%)
υ_{62}	325	0	2	315	334	330			τ_{CCCH}(11%)+τ_{CCCC}(10%)
υ_{63}	303	0	1	299	308	305		285	δ_{CCH}(21%)+τ_{CNSO}(19%)+δ_{CSO}(13%)
υ_{64}	268	1	0	266	272	269			τ_{CCCH}(16%)+τ_{CCCC}(12%)+δ_{CCC}(11%)
υ_{65}	193	0	0	190	198	196			τ_{CCSO}(24%)+δ_{CNS}(15%)
υ_{66}	192	1	3	190	196	193			τ_{CNSO}(18%)+τ_{CCCH}(18%)+τ_{CCCC}(13%)+τ_{CCNS}(10%)+τ_{CNHS}(10%)
υ_{67}	153	1	2	152	156	154			τ_{CNSO}(28%)+τ_{CCSO}(17%)+δ_{CCS}(10%)
υ_{68}	101	1	0	100	104	102			τ_{CNSO}(15%)+τ_{CNSH}(12%)+τ_{CCNS}(10%)+τ_{CCCC}(10%)+τ_{CCCH}(10%)
υ_{69}	57	0	0	59	56	57			τ_{CCCH}(32%)+τ_{CNSO}(30%)+τ_{CCSO}(16%)+τ_{CCNS}(11%)
υ_{70}	40	0	1	39	41	41		46	τ_{CCNS}(20%)+τ_{CNSO}(16%)+τ_{CNSH}(13%)

(*continued on next page*)

Table 2 (*continued*)

Mode no	Theoretical (B3LYP)						Experimental		%TED[d]
	6-311 G(d,p)			cc-pVDZ	cc-pVQZ	cc-pVTZ	FT-IR	FT-Raman	
	Freq[a]	I_{IR}[b]	I_{Raman}[c]	Freq[a]	Freq[a]				
υ_{71}	32	0	2	34	32	32			τ_{CCCH}(68%)
υ_{72}	24	0	3	24	21	24			τ_{CCCH}(82%)

υ: stretching, δ: in-plane bending, γ: out-of plane bending τ: torsion.
[a] Obtained from the wave numbers calculated at 0.967 for 6-311G(d,p), 0.970 for cc-pVDZ, 0.965 for cc-pVTZ, 0.969 for cc-pVQZ.
[b,c] Relative absorption intensities and Relative Raman intensities normalized with highest peak absorption equal to 100.
[d] Total energy distribution calculated B3LYP/6-311 G(d,p) level of theory. Only contributions 10% are listed.

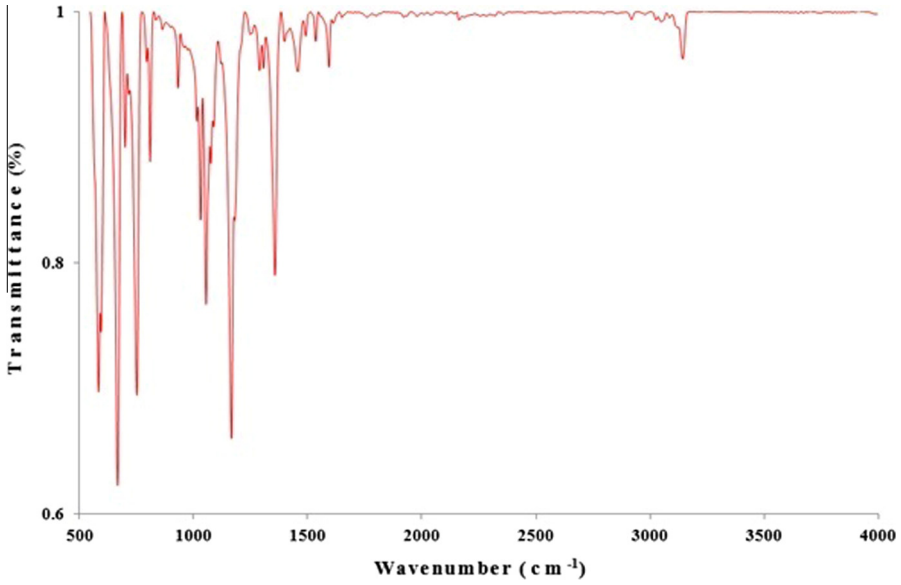

Fig. 2a. Experimental FT-Infrared Spectra of 1PTSP molecule.

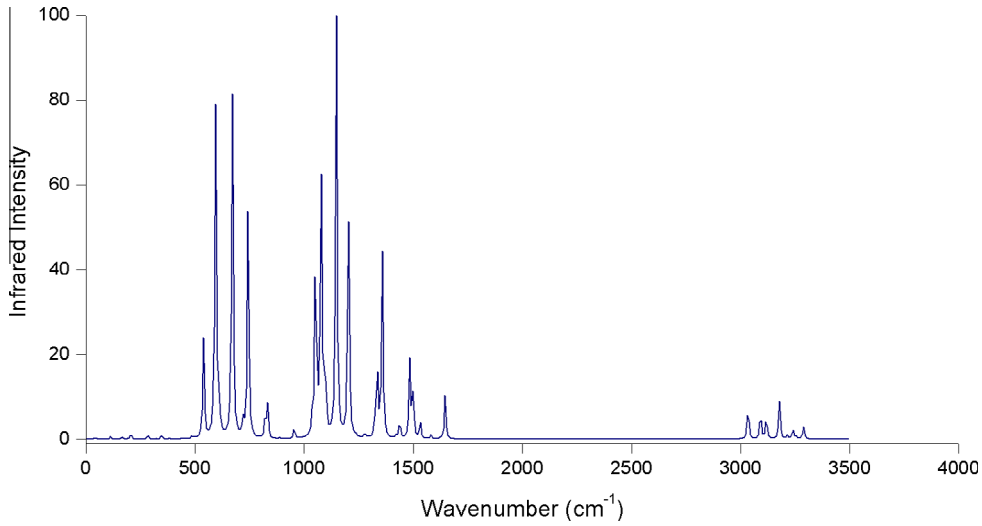

Fig. 2b. Theoretical infrared spectra of 1PTSP molecule.

2982 cm^{-1} bands predicted were assigned to the asymmetric CH_3 stretching vibrations by B3LYP/6-311 G(d,p) level of theory. These bands could not detected by experimental procedure. But, observed CH_3 symmetric stretching vibrations at 2920 cm^{-1} (Raman) corresponds to the calculated wavenumber at 2927 cm^{-1} by B3LYP/6-311 G(d,p) level of theory. The CH and CH_3 calculated values are in good agreement with the experimental data.

The asymmetric deformations vibration of the CH_3 group were founded at 1474 cm^{-1} (DFT)//1459 cm^{-1} (IR)//1461 cm^{-1} (Raman) by using theoretical and experimental procedure. The symmetric deformation vibration of the CH_3 group was predicted at 1369 cm^{-1} by DFT. But, this vibration could not to be observed by experimental spectra. In the earlier work, methyl rocking vibrations determined [23,24] in the region 1150–925 cm^{-1}. According

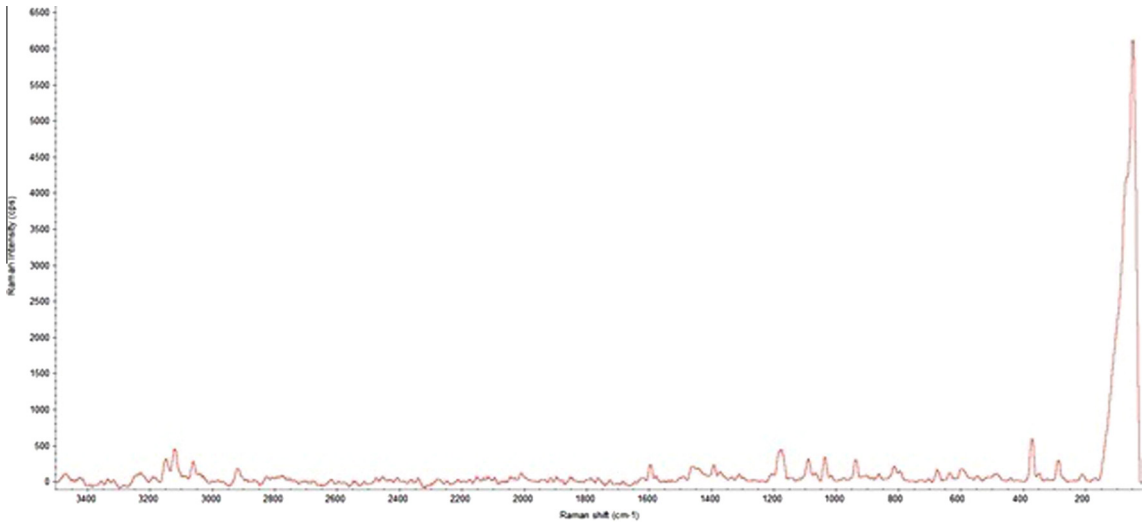

Fig. 3a. Experimental FT-Raman spectra of 1PTSP molecule.

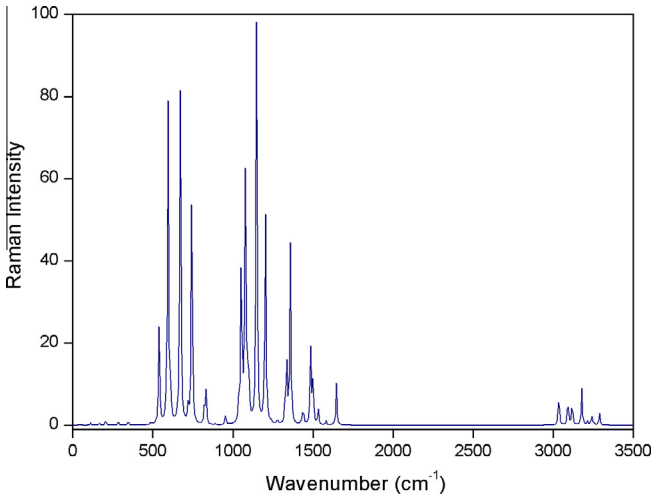

Fig. 3b. Theoretical FT-Raman spectra of 1PTSP molecule.

to our calculations, The DFT calculations computed the rocking modes of the methyl group at 1028 and 977 cm^{-1}.

C–C vibrations

In a pyrrole ring, the Carbon–Carbon bond-stretching mode has been observed at 1546 cm^{-1} in infrared spectrum by Singh et al. [25]. In 1PTSP molecule, 1537 cm^{-1} band was assigned to the CC stretching modes by FT-IR spectra. This mode was calculated at 1522 cm^{-1} by using B3LYP/6-311 G(d,p) level of theory. The C–C stretch of the phenyl group (ν_{61}) for the ground state was predicted to be medium band (11 km mol^{-1}) in the infrared spectrum at 1594 cm^{-1} but it has only 39% contribution. Corresponding mode has been detected at 1594 cm^{-1} for FT-Raman spectra. Other one (ν_{61}) has been calculated at 1562 cm^{-1} but, it was not measured by using the experimental techniques.

S=O vibrations

The $\upsilon_{S=O}$ group has two stretching modes, which are symmetric and asymmetric stretching vibrations. One of them founded as a very strong band at 1103 cm^{-1} in the DFT calculation and at 1087 cm^{-1} in the Raman spectrum has been assigned to the symmetric $\upsilon_{S=O}$ stretching vibration. The other peak which is asymmetric $\upsilon_{S=O}$ vibration observed at 1309 cm^{-1} in the infrared spectrum and computed at 1306 cm^{-1} by B3LYP/6-311G(d,p) level of theory. Peak computed at 1156 cm^{-1} in the B3LYP//6-311 G(d,p) level of theory was assigned to the ν_{SO2-N} stretching vibration but it was not measured by experimental procedure. In the studied molecule, 1594 cm^{-1} observed band (both FT-IR and FT-Raman spectra) was assigned to CC stretching mode. This mode was predicted 1584 cm^{-1} by 6-311 G(d,p) basis set calculation.

NMR spectra

In this calculations, chemical shifts value were predicted by "Gauge-Independent Atomic Orbital" (GIAO) approximation at IEF-PCM model (DMSO solution). The Nuclear Magnetic Rezonans spectra of the ground state geometry of 1PTSP molecule have been obtained by DFT/GIAO method. The GIAO method is one of the

Table 3
The observed and predicted ^{1}H and ^{13}C NMR isotropic chemical shifts of 1-(p-tolylsulfonyl) pyrrole (with respect to TMS, all values in ppm).

Atom numbering	Theoretical (B3LYP)				Experimental
	6-311 G(d,p)	cc-pVDZ	cc-pVTZ	cc-pVQZ	
H_{16}	7.83	8.09	8.40	8.53	7.8
H_{17}	7.83	8.09	8.40	8.53	7.8
H_{20}	7.54	7.71	7.93	8.04	7.4
H_{21}	7.54	7.71	7.93	8.04	7.4
H_{18}	7.04	7.33	7.65	7.79	7.3
H_{19}	7.04	7.33	7.65	7.79	7.3
H_{22}	6.36	6.60	6.80	6.93	6.3
H_{23}	6.36	6.60	6.80	6.93	6.3
H_{25}	2.54	2.84	2.89	2.97	2.6
H_{26}	2.30	2.56	2.70	2.78	2.5
H_{24}	2.30	2.56	2.70	2.78	2.5
C_8	153.6	137.0	154.9	161.0	145.8
C_5	145.2	131.6	146.2	151.9	135.8
C_{11}	134.4	118.4	135.0	140.1	130.7
C_{12}	134.4	118.4	135.0	140.1	130.7
C_6	130.4	114.7	131.9	137.3	127.1
C_7	130.4	114.7	131.9	137.3	127.1
C_{10}	122.0	106.5	122.6	128.5	121.4
C_9	122.0	106.5	122.6	128.5	121.4
C_{14}	116.2	99.79	116.5	121.5	114.2
C_{13}	116.2	99.79	116.5	121.5	114.2
C_{15}	22.12	24.20	24.4	25.06	21.5

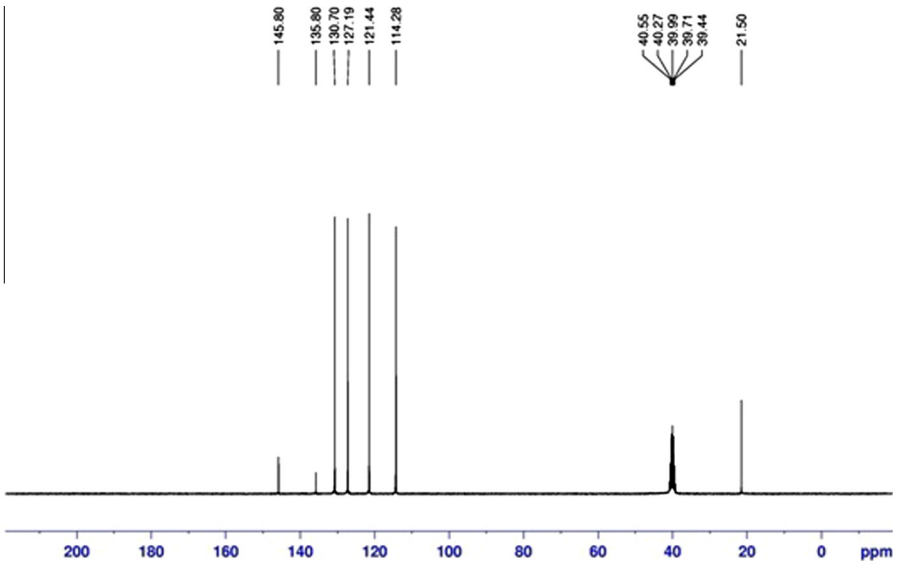

Fig. 4. ^{13}C NMR spectrum of 1PTSP molecule.

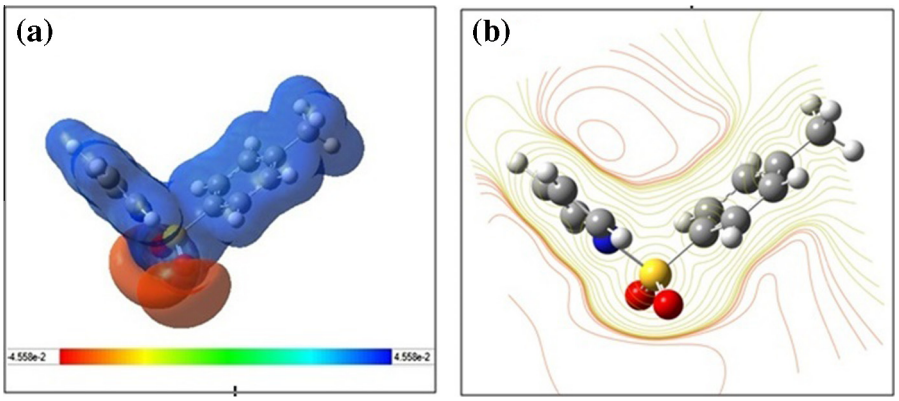

Fig. 5. Calculated 3D molecular electrostatic potential (a) and contour diagram (b) for 1PTSP molecule calculated at the B3LYP/-311 G(d,p).

most common methods for calculating isotropic nuclear magnetic. The predicted and measured NMR values were listed in Table 3.

As seen in Fig. 4, the ^{13}C NMR chemical shifts usually are larger than 100 ppm [26–28]. There are 11 NMR signals in the corresponding spectrum of 1PTSP. The carbon NMR signals for aromatic rings were observed at 145.8–114.2 ppm. Six (C_8, C_5, C_{11}, C_{12}, C_6 and C_7) of them are carbon atoms of the methyl group. Four of them are carbon atoms (C_{10}, C_9, C_{14} and C_{13}) of the pyrrole group. Other one is carbon atom (C_{15}) of the methyl group.

Hydrogen, which attached methyl group can decrease the shielding and move the resonance of attached proton towards to a higher frequency. C_8, which is bonded methyl group, determined at 153.6 ppm (experimental) and 145.8 ppm (B3LYP/6-311 G(d,p) level of theory). Carbon signals of the other phenyl group were determined at 135.8/145.2 ppm (C_5), 130.7/134.4 ppm (C_{11} and C_{12}), 127.1/130.4 ppm (C_6 and C_7) by using experimental and DFT results. The chemical shifts of the pyrrole group are smaller than those of phenyl group. NMR signals of the pyrrole group were founded at 121.4 ppm (C_9 and C_{10} atoms) and 114.2 ppm (C_{14} and C_{13} atoms) by means of ^{13}C NMR spectra. These were predicted at 122.0 ppm (C_9 and C_{10} atoms) and 116.2 ppm (C_{14} and C_{13} atoms) by B3LYP/6-311 G(d,p) level of theory. The NMR signal of Carbon-15 atom is smaller than the other aromatic carbons due to the methyl group. C_{15}, which is the methyl group, resonates in the highest field (21.5 ppm) and shows a quite good correlation with theoretical value of 22.12 ppm.

The NMR signals of proton, which is bounded to CH_3 group, are appeared towards higher magnetic field. All of them have been computed and detected as quite low. Because, the CH_3 groups are usually displayed as electron forgiven groups, so they will be more shielded. All hydrogen atoms of methyl group chemical shift values are lower than 3 ppm because of the shielding effect. H_{24}, H_{25} and H_{26} chemical shifts were determined at 2.6, 2.4 and 2.4 ppm. According to the NMR spectra, the NMR signals of hydrogen atom, which are attached benzene group, were detected at 7.8 ppm and 7.4 ppm. Besides, the chemical shifts chemical shifts of hydrogen atoms of pyrrole group have been experimentally observed at 7.3–6.3 ppm. H_{18}–H_{19} and H_{22}–H_{23} protons are equivalent protons. As seen in Table 3, experimental NMR spectra of 1PTSP molecule are in excellent agreement with theoretical ones.

Molecular electrostatic potential (MEP)

The molecular electrostatic potential (MEP) is concerned with the electronic density. It is produced by the nuclei and the electrons. It is especially used for determining corresponding sites for electrophilic–nucleophilic reactions and hydrogen-bonding interactions. It is demonstrated that the negative potential sites are on electronegative atoms. It is also showed that the positive potential located on the hydrogen atoms. These regions give knowledge about whether the molecule has inter-molecular interplays. In

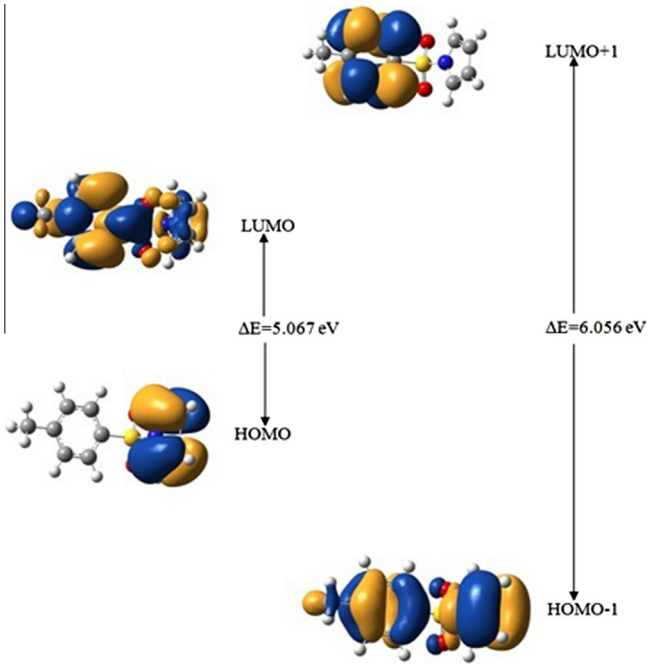

Fig. 6. HOMO LUMO plot of 1PTSP molecule by B3LYP/6-311 G(d,p) level of theory.

Table 4
Calculated some properties values of 1PTSP molecule in its ground state.

	Conformer-1
E_{HOMO} (eV)	−6.636
E_{LUMO} (eV)	−1.569
E_{GAP} (eV)	5.067
E_{HOMO-1} (eV)	−7.112
E_{LUMO+1} (eV)	−1.056
I_P (eV)	6.636
E_A (eV)	1.569
η (eV)	2.533
χ (eV)	4.102
Dipole moment (D)	
μ_{total}	−4.115
μ_x	3.701
μ_y	−0.000
μ_z	5.534

other words, it can be used for determining the possible sites for electrophilic attack and nucleophilic reactions. It also can be used for the reactive behavior of chemical systems, biological recognition processes and hydrogen bonding interactions [29–33].

Electrostatic potential map shown in Fig. 5 illustrates the 3D charge distributions of the molecule. As seen in Fig. 5, the electrostatic potential at the surface was showed by different colors. While blue regions evidenced to the most positive electrostatic potential, the most electronegative electrostatic potential was symbolized as a red color. In addition, the other color is green, which is shown zero potential regions. The ranking of the electrostatic potential is red < orange < yellow < green < blue. According to the corresponding results, the MEP map predicted that the negative potential sites are on oxygen atoms and the positive potential sites are around the hydrogen atoms.

HOMO–LUMO energies

HOMO energy, which is Highest Occupied Molecular Orbital, and LUMO energy, which is Lowest Unoccupied Molecular Orbital of 1PTSP molecule were computed by means of B3LYP/6-311 G(d,p) level of theory. The plotted HOMO and LUMO were illustrated in Fig. 6.

It is note that the HOMO is located on the all pyrrole and SO_2 groups, while LUMO is located on whole molecule. The computed HOMO–LUMO energy gap of 1PTSP molecule has been founded at 5.067 eV. In the Koopman's theorem, the electron affinity, ionization potential, chemical hardness and electronegativity can be calculated by means of their energy values [34–36].

$$I_P \approx -I_P \approx -E_{HOMO}$$

$$E_A \approx -E_A \approx -E_{LUMO}$$

$$\eta = \left(\frac{E_{LUMO} - E_{HUMO}}{2}\right) \text{ or } \eta = (I_P - E_A)/2,$$

$$\chi = \left(\frac{E_{LUMO} - E_{HUMO}}{2}\right) \text{ or } \chi = (I_P - E_A)/2.$$

In the gas phase of the 1PTSP molecule, E_A and I_P were computed at 6.636 eV, 1.569 eV, respectively. The calculated results were listed in Table 4. Chemical hardness can relate the stability of molecule. In other words, it can be showed that a molecule, which has lower chemical hardness, is more reactive [34–36]. Chemical hardness of the 1PTSP molecule were computed at 2.533 eV by B3LYP/6-311 G(d,p) level of theory.

Conclusion

This investigation proves that the vibrational spectra, conformational analysis, Nuclear Magnetic Resonance spectra and molecular structure of 1PTSP molecule by combining theoretical and experimental studies. The conformational properties can be successfully predicted by MMFF approach. We determined the most stable conformer of the 1PTSP by combining DFT and MMFF approaches. The lowest energy conformers of 1PTSP obtained according to the above methodology were further studied using the Density Functional Theory at B3LYP/6-311G** level. The spectroscopic, structural and electronic properties of the most stable conformer have been calculated by Gaussian software. Especially, vibrational spectrum of 1PTSP (powder form) has been extensively investigated for the first time by means of both experimentally and quantum chemical calculations. The experimental work has focused on the assignment of the vibrational energy levels from 400 to 4000 cm^{-1}. Computed results of the most stable conformer were found to be in better agreement with the experimental findings.

Acknowledgements

Y. Erdogdu acknowledges computing resources support from the National Center for High Performance Computing of Ahi Evran University (AHILAB).

References

[1] D.L. Wise, G.E. Wirek, D.J. Trantolo, T.M. Cooper, J.D. Gresser, Electrical and Optical Polymer Systems, vol. 17, Marcel Dekker, New York, 1998.
[2] J. Rodriquez, H.J. Grande, T.F. Otero, in: H.S. Nalwa (Ed.), Handbook of Organic Conductive Molecules and Polymers, John Wiley & Sons, New York, 1997.
[3] J. Simonet, J.R. Berthelot, Prog. Solid State Chem. 21 (1991) 1.
[4] A.F. Diaz, J. Bargon, in: T.A. Skotheim (Ed.), Handbook of Conducting Polymers, vol. I, Dekker, New York, 1986.
[5] B.B. Snider, S.B. Neubert, J. Org. Chem. 69 (2004) 8952.
[6] Z. Feng, X. Li, G. Zheng, L. Huang, Bioorg. Med. Chem. Lett. 19 (2009) 2112.
[7] C. Alp, D. Ekinci, M.S. Gultekin, M. Şenturk, E. Şahin, Ö.İ. Kufrevioğlu, Bioorg. Med. Chem. 18 (2010) 4468.
[8] R.N. Singh, P. Rawat, A. Kumar, J. Mol. Struct. 1061 (2014) 140.
[9] K.L. Nelson, in: G.A. Olah (Ed.), Friedel-Crafts and related reactions, Wiley, New York, 1964, p. 1024.

[10] M.J. Frisch et al., Gaussian 09, Revision B.01, Gaussian Inc., Wallingford CT, 2010.
[11] H.B. Schlegel, J. Comput. Chem. 3 (1982) 214.
[12] T.A. Halgren, J. Comput. Chem. 17 (1996) 490–519.
[13] G. Rauhut, P. Pulay, J. Phys. Chem. 99 (1995) 3093.
[14] Spartan 10 Wavefunction Inc., Irvine, CA 92612, USA, 2010.
[15] R.N. Singh, P. Rawat, A. Kumar, J. Mol. Struct. 1061 (2014) 140.
[16] S. Subashchandrabose, H. Saleem, Y. Erdogdu, Ö. Dereli, V. Thanikachalam, J. Jayabharathi, Spectrochim. Acta Part A 86 (2012) 231.
[17] N.P.G. Roeges, A Guide to the Complete Interpretation of Infrared Spectra of Organic Compounds, Wiley, New York, 1994.
[18] S. Kalaichelvan, N. Sundaraganesan, Ö. Dereli, U. Sayin, Spectrochim. Acta Part A 85 (2012) 198.
[19] N. Subramaniana, N. Sundaraganesanc, Ö. Dereli, E. Türkkan, Spectrochim. Acta Part A 83 (2011) 165.
[20] E.K. Sarıkaya, Ö. Dereli, J. Mol. Struct. 1052 (2013) 214.
[21] Ö. Dereli, S. Sudha, N. Sundaraganesan, J. Mol. Struct. 994 (2011) 379.
[22] D. Sajan, Y. Erdogdu, R. Reshmy, Ö. Dereli, K. Kurien Thomas, I. Hubert Joe, Spectrochim. Acta Part A 82 (2011) 118.
[23] N.P.G. Roeges, A Guide to the Complete Interpretation of Infrared Spectra of Organic Structures, Wiley, New York, 1994.
[24] V. Schettino, G. Sbrana, R. Righini, Chem. Phys. Lett. 13 (1972) 284.
[25] R.N. Singh, A. Kumar, R.K. Tiwari, P. Rawat, V.P. Gupta, J. Mol. Struct. 1035 (2013) 427.
[26] Y. Erdogdu, S. Saglam, J. Mol. Struct. 1061 (2014) 140.
[27] H. Saleem, A.R. Krishnan, Y. Erdogdu, S. Subashchandrabose, V. Thanikachalam, G. Manikandan, J. Mol. Struct. 999 (2011) 2.
[28] Y. Erdogdu, Spectrochim. Acta Part A 106 (2013) (2013) 25.
[29] I. Alkorta, J.J. Perez, Int. J. Quantum Chem. 57 (1996) 123.
[30] E. Scrocco, J. Tomasi, in: P. Lowdin (Ed.), Advances in Quantum Chemistry, vol. 2, Academic Press, New York, 1978.
[31] F.J. Luque, M. Orozco, P.K. Bhadane, S.R. Gadre, J. Phys. Chem. 97 (1993) 9380.
[32] J. Sponer, P. Hobza, Int. J. Quantum Chem. 57 (1996) 959.
[33] J.S. Murray, K. Sen, Molecular Electrostatic Potentials, Concepts and Applications, Elsevier, Amsterdam, 1996.
[34] T.A. Koopmans, Physica 1 (1933) 104.
[35] C.G. Zhan, J.A. Nichols, D.A. Dixon, J. Phys. Chem. A 107 (2003) 4184.
[36] L. Joseph, D. Sajan, R. Reshmy, B.S. ArunSasi, Y. Erdogdu, K.K. Thomas, Spectrochim. Acta Part A 99 (2012) 234.